Synthesis of Averaged Circuit Models for Switched Power Converters

Seth R. Sanders and George C. Verghese

Abstract —Averaged circuit models for switching power converters are useful for analysis and simulation, and for obtaining engineering intuition into the operation of these switched circuits. This paper develops averaged circuit models for switching converters using a direct circuit averaging method. The method proceeds in a systematic fashion by determining appropriate averaged circuit elements that are consistent with the averaged circuit waveforms. The averaged circuit models that are obtained are syntheses of the state-space averaged models for the underlying switched circuits. An important feature of our method is that it is applicable to switched circuits whose non-switch elements may be nonlinear. Our approach is compared and contrasted with the results on averaged circuit models currently available in the literature.

I. INTRODUCTION

THIS paper studies the existence and synthesis of non-switched circuits that exhibit the dynamics described by the state-space averaged model of a given switching power converter. An averaged circuit representation for a switching converter is useful for analysis, for circuit-based simulation, and for obtaining engineering intuition into the operation of the switching converter. In order that the averaged circuit be most useful, it is desired that this model resemble as closely as possible the underlying switched circuit. The method of *in-place* or direct circuit averaging pioneered by Wester and Middlebrook [18] is a natural approach for obtaining averaged circuit models. With this method, one attempts to replace each element of the switched converter circuit by an appropriate "averaged element." The main contribution of this paper is in extending the earlier results of [18] (and others) on averaged circuit synthesis. In particular, we give a systematic approach for synthesizing averaged circuit models that realize their respective state-space averaged models. Our synthesis procedure, unlike

earlier work, is applicable to switched circuits whose non-switch elements may be nonlinear.

The paper is organized as follows. Section II presents background on modeling of switching power converters; an up–down converter is used as the main example in that section and in the remainder of the paper. Undoubtedly, the ideas developed in this paper are applicable to other areas where switched circuits are used, but we focus our attention on switching power converters since this application area motivated our research. As mentioned above, there has been significant previous work on the synthesis of averaged circuit models. We give a brief summary of previous work in Section III. The relationships between our results and previous ones are also discussed as our development proceeds. Our main results on averaged circuit synthesis are contained in Section IV along with a number of examples. Summarizing remarks are included in Section V.

II. STATE-SPACE MODELS FOR POWER ELECTRONIC CIRCUITS

This section develops a state-space model for an up–down converter to illustrate the nature of state-space models for power electronic circuits. This model and certain variants of it are used extensively as examples in the remainder of the paper. For more details on modeling of power electronic circuits; see [1]–[3], [20].

Consider the up–down converter shown in Fig. 1(a). The nominal steady-state operation of such a converter involves a cyclic process. The transistor is turned on in the first part of the cycle, so that the inductor current ramps up. During this time, the diode is reverse biased (a nonconducting state) so that the capacitor voltage decays into the load. Then, in the second part of the cycle, the transistor is turned off and the diode becomes forward biased (a conducting state), so that the inductor current flows through the diode into the capacitor and the load. Typical waveforms are displayed in Fig. 1(b). The switching frequency is invariably picked high enough to yield a small switching ripple.

With this type of cyclic operation, the average value of the capacitor voltage v in the steady state can be made either larger or smaller in magnitude than the source voltage V_s. This is why the circuit is termed an *up–down converter*. Note also that if the transistor and diode func-
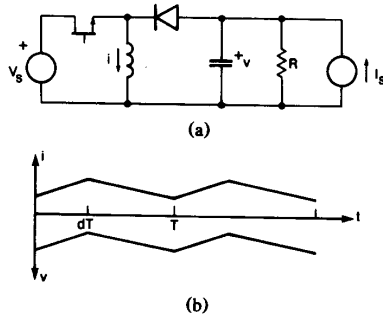
Fig. 1. (a) Up–down converter. (b) Typical waveforms.

tion essentially as ideal switches, then the power dissipation is mainly in the load, i.e., the converter operates at high efficiency. One can determine the approximate steady state transfer ratio from source voltage to average capacitor voltage by noting that the average voltage across the inductor is zero in steady state, and hence

$$(d)V_s + (1-d)v_n \approx 0 \tag{1}$$

where v_n is the nominal steady state value of the capacitor voltage and d is the *duty ratio*, that is, the fraction of each cycle that the transistor is on. From (1), we readily obtain

$$v_n \approx -\frac{d}{1-d}V_s. \tag{2}$$

Under the restriction that the inductor current i is always positive (so-called continuous conduction), we can model the transistor-diode pair as a single pole, double throw (SPDT) switch. Note that the position of the switch can always be dictated by turning the transistor on ($u = 1$) or off ($u = 0$). When either switch position is specified, the circuit can be characterized by a linear, time-invariant (LTI) model. Suppose that under $u = 1$, a state-space model is given by

$$x' = A_1 x + B_1 w \tag{3}$$

and under $u = 0$, is given by

$$x' = A_0 x + B_0 w \tag{4}$$

where x is a state vector comprising the capacitor voltage and the inductor current, x' is its time derivative, and w is the vector of voltage and current source values. Note that we have not explicitly noted the time dependence in the state x and its derivative x', and we shall continue this omission throughout the paper when such dependence is clear from the context. An ensemble model in bilinear form can be obtained by combining (3) and (4) as

$$x' = [A_0 + u(A_1 - A_0)]x + [B_0 + u(B_1 - B_0)]w. \tag{5}$$

For the up–down converter of Fig. 1, the state-space

representation takes the form

$$\begin{bmatrix} i' \\ v' \end{bmatrix} = \left\{ \begin{bmatrix} 0 & 1/L \\ -1/C & -1/RC \end{bmatrix} + u \begin{bmatrix} 0 & -1/L \\ 1/C & 0 \end{bmatrix} \right\} \begin{bmatrix} i \\ v \end{bmatrix}$$
$$+ u \begin{bmatrix} V_s/L \\ 0 \end{bmatrix} + \begin{bmatrix} 0 \\ I_s/C \end{bmatrix}. \tag{6}$$

Note that the control variable u takes on only the values 0 and 1.

In the more general case where nonlinear circuit elements are present in a switching converter, the ensemble model (5) would take the more general form

$$x' = f_0(x) + u[f_1(x) - f_0(x)]. \tag{7}$$

Terms corresponding to independent sources may be absorbed into $f_0(\cdot)$ and $f_1(\cdot)$ in (7). In some applications involving time-varying source and/or load waveforms, the vector-valued functions $f_0(\cdot)$ and $f_1(\cdot)$ may be time dependent. For all cases of interest in this paper, $f_0(\cdot)$ and $f_1(\cdot)$ will be continuous functions of their arguments.

There are many converters of interest that admit more than two switch configurations. For details on modeling these converters and on deriving averaged circuit representations, see [31].

State-Space Averaged Models: To facilitate the use of well-established control design methods based on state-space models that have a continuously variable input, *state-space averaged* models for switching converters have been developed [4], [5], [20]. A state-space averaged model is an approximation to a model that contains discrete control inputs (such as (6)), and can be obtained by replacing the instantaneous values of all state and control variables by their one-cycle averages, i.e.,

$$\bar{x}(t) = \frac{1}{T} \int_{t-T}^{t} x(s)\,ds \tag{8}$$

$$d(t) = \bar{u}(t) = \frac{1}{T} \int_{t-T}^{t} u(s)\,ds \tag{9}$$

in the case where the converter is operated cyclically with period T. The symbol d is used to represent the duty ratio, that is, the one-cycle averaged value of u. See [18] and [20] for discussions on the use of one-cycle averaging for developing state-space averaged models.

To develop some intuition on the approximations involved, consider applying the one-cycle average to the model (7). We obtain

$$\bar{x}' = \overline{f_0(x)} + \overline{u[f_1(x) - f_0(x)]}. \tag{10}$$

Note that the one-cycle averaging operation commutes with differentiation (as demonstrated in Section IV), and hence the left-hand side of (10) is equal to $\bar{x}'$. Under the conditions that the states do not vary much over any interval of duration T (small ripple assumption), and that the functions $f_0(\cdot), f_1(\cdot)$ are continuous, the right-hand side of (10) can be approximated as

$$f_0(\bar{x}) + d[f_1(\bar{x}) - f_0(\bar{x})] \tag{11}$$

for small enough T. This approximation can be justified by first noting that the small ripple and continuity condi-

SANDERS AND VERGHESE: SYNTHESIS OF AVERAGED CIRCUIT

tions assure that the relative variation in the functions $f_0(\cdot), f_1(\cdot)$ is small over the interval of duration T, and hence

$$\overline{u[f_1(x) - f_0(x)]} \approx \bar{u}\overline{[f_1(x) - f_0(x)]}$$

$$= d\overline{[f_1(x) - f_0(x)]}. \quad (12)$$

The small ripple and continuity conditions also permit the approximations

$$\overline{f_0(x)} \approx f_0(\bar{x})$$

$$\overline{f_1(x)} \approx f_1(\bar{x}) \quad (13)$$

which lead to our result. (Note that in the case where the functions $f_0(\cdot), f_1(\cdot)$ are linear or affine, (13) involves no approximation.) In summary, the state-space averaged model for (7) takes the form

$$\bar{x}' = f_0(\bar{x}) + d[f_1(\bar{x}) - f_0(\bar{x})]. \quad (14)$$

Note that this type of averaging is used in many disciplines in the systems and control literature including convergence analysis of adaptive control schemes (e.g., [28]) and sliding mode control (e.g., [6]). For the up–down converter, the state-space averaged model has an identical form to that of (6), except that the discrete input u is replaced with the continuous duty ratio d, which can take on any value satisfying $0 \leqslant d \leqslant 1$. In the remainder of the paper, we shall omit (except where otherwise indicated) the overbar notation when considering state-space averaged models, to simplify the presentation. The nature of the model of interest should be clear from the context.

In the case where the functions $f_0(\cdot)$ and $f_1(\cdot)$ possess bounded and continuous first partial derivatives with respect to x, the trajectories of the averaged model can be shown to approximate those of the underlying switched system model on a finite interval with arbitrarily small error, for sufficiently small T. See [28], [29], and [37] for results of this type. Also see [4], [5], and [13] for discussions of the approximations involved in averaging. References [28] and [37] also essentially prove that the underlying switched system is exponentially stable for all sufficiently small T if the state-space averaged system is exponentially stable. Our focus in this paper is not on the approximations involved in averaging, but on the relationship between state-space averaged models and circuit realizations for these. Therefore, we omit further discussion of the approximations involved in averaging. For a preview of our results, see Fig. 5, which shows a circuit realization of the state-space averaged model of a variation of our up–down converter.

A control law $d = -h(\bar{x})$ designed using the state-space averaged model is typically implemented in the switched system by comparing the quantity $h(x)$ to a ramp waveform $r(t)$ of the form shown in Fig. 2. The switched control law might then take the form

$$u = \begin{cases} 1, & h(x) < r(t) \\ 0, & h(x) \geqslant r(t). \end{cases} \quad (15)$$

Fig. 2. Ramp waveform used to implement control based on state-space averaged model.

III. PREVIOUS WORK ON AVERAGED CIRCUITS

The earliest work on averaged circuit models for switching converters was that of Wester and Middlebrook [18]. In [18], the technique used to obtain an averaged circuit realization for a given switching converter could be termed an *in-place* averaging scheme, where the averaging is performed directly on the circuit. In particular, [18] suggested the construction of an averaged circuit model whose branch variables are one-cycle averages (see Section II) of the corresponding branch variables of the underlying switched circuit. This very physical approach results in an averaged circuit that closely resembles the underlying circuit. However, [18] did not adequately realize the elements required to replace the switch branches. Rather, each ideal switch pair was simply replaced by an ideal transformer. A consequence of this is that the state-space model that governs the dynamics of the obtained averaged circuit is not always equivalent to the state-space averaged model for the underlying switched circuit. The later averaged circuit synthesis method of Middlebrook and Cuk [5], [13], termed "hybrid modeling," is based on the state-space averaged model (and proceeds apparently by inspection). This technique results in circuit syntheses that do indeed realize the state-space averaged models for their underlying models. The development by Cuk and Middlebrook in [21] illustrated an analogous approach for synthesizing averaged circuits for switching converters operating in the discontinuous conduction mode. It is claimed in [5], [13], and [21] that the technique is applicable to any converter; however, syntheses are only given for a set of example converters.

The recent work of Vorperian [15], [16] and Tymerski *et al.* [14] follows the in-place averaging approach in constructing averaged circuit models. Reference [15] does adequately realize the elements needed to replace the switch branches when parasitic effects such as equivalent series resistance (ESR) are present. Reference [16] develops a model for operation in the discontinuous conduction mode that is essentially different from other existing models. More discussion of this will be given in Section 4.2. The paper of Lee [17] also has many similar ideas and results.

Some recent publications have extended the in-place averaging approach to quasi-resonant type circuits. See [33] and [34] for details on this development. Another challenge is the development of averaged circuit models for the resonant type converters. Some results in this direction can be found in [32], [35], [36], and [38].

Averaged circuit models have also been developed for the analysis of switched-capacitor filters. In particular, the

paper of Tsividis [22] illustrates the replacement of a capacitor and switch pair by a simple resistor. This equivalent circuit modeling involves a reduction of the order of the state-space, as is required in modeling a switching converter operating in the discontinuous conduction mode. Similar ideas were applied by other authors [23], [24] for the analysis of switched-capacitor circuits.

Fig. 3. Partitioned switching converter.

IV. AVERAGED CIRCUIT SYNTHESIS VIA IN-PLACE AVERAGING

The in-place averaging method is based on the application of the one-cycle averaging operation to each branch variable in a switched circuit, e.g.,

$$\bar{i}(t) = \frac{1}{T}\int_{t-T}^{t} i(s)\, ds \tag{16}$$

for some branch current where the averaging interval T is selected to be equal to the fundamental period of the cyclic operation of the switches. A fundamental property of the resulting averaged branch variables is that these variables satisfy the same topological constraints, namely Kirchhoff's current and voltage laws (KCL and KVL), as the respective variables in the nonaveraged circuit. This follows from the facts that the constraints imposed on the circuit branch variables by KCL and KVL are inherently linear algebraic constraints, and apply identically at each time instant. A first step in the synthesis of an averaged circuit is then to consider a circuit that is topologically equivalent to the underlying switched circuit. In order to complete the synthesis, we need to specify averaged circuit elements that are consistent with the one-cycle averaged branch variables.

The reactive elements of the underlying circuit are preserved intact in the averaged circuit. To see why, we can consider without loss of generality a nonlinear multiport capacitor, represented by the state-space description

$$q' = i$$

$$v = f(q) \tag{17}$$

where $f(\cdot)$ (assumed to be continuous) is the gradient of a scalar function, i.e., $f(q) = \nabla W(q)$ where $W(q)$ is the internal energy of the capacitor to within an additive constant. Consider the application of the one-cycle averaging operation (16) to this element. The averaging operation commutes with differentiation with respect to time since

$$\bar{q}'(t) = \frac{d}{dt}\frac{1}{T}\int_{t-T}^{t} q(s)\, ds = \frac{q(t) - q(t-T)}{T}$$

$$= \frac{1}{T}\int_{t-T}^{t} q'(s)\, ds = \overline{q'(t)} \tag{18}$$

and therefore, we have $\bar{q}' = \bar{i}$. In general, $\bar{v} \neq f(\bar{q})$. However, for continuous waveforms and for continuous $f(\cdot)$ in (17), the approximation $\bar{v} \approx f(\bar{q})$ approaches equality arbitrarily closely for sufficiently small T. This approxima-
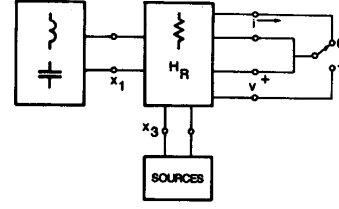
tion is identical to that made in state-space averaging [4], [5] in the context of state-space models for power circuits.

The linear resistive elements and sources of the underlying circuit are also preserved intact in the averaged circuit, which can be demonstrated by the application of the one-cycle averaging operation to the terminal waveforms of these elements. The following two subsections treat the respective cases where only LTI resistive elements are present in the circuit and where nonlinear resistive elements may be present.

4.1. Averaged Circuit Synthesis with LTI Resistive Elements

The preceding discussion motivates the following theorem for circuits built from LTI resistive elements, ideal sources, and one controlled switch. The theorem refers to a circuit partitioned as in Fig. 3, and requires the following two assumptions.

Assumption 4.1: Each branch voltage and each branch current in the underlying switching converter circuit has a unique solution corresponding to each value of the state vector of capacitor charges (or voltages) and inductor fluxes (or currents).

Assumption 4.2: There exists a hybrid representation for the resistive multiport (H_R) in Fig. 3 with controlling port variables taken as currents for those ports connected to current source or inductive ports, as voltages for those ports connected to voltage source or capacitive ports, and with exactly one current-controlled switch port and one voltage-controlled switch port.

Theorem 4.1: Suppose Assumptions 4.1 and 4.2 hold, then an averaged circuit model for the partitioned circuit of Fig. 3 can be obtained by replacing the two-port switch network with a resistive two-port with hybrid representation

$$H_s(d) = \frac{d}{1-d} H_{22} \tag{19}$$

for $d \neq 1$, where H_{22} is the hybrid immittance seen by the switch two-port when all current source and inductive branches are replaced by open circuits and all voltage source and capacitor branches are replaced by short circuits. (The switch positions must be labeled so that $u = 0$ corresponds to the position where the current-controlled
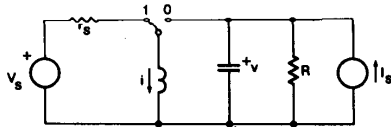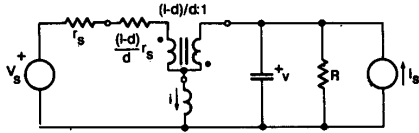
Fig. 4. Up–down converter with source resistance.

Fig. 5. Averaged circuit for up–down converter with source resistance.

Fig. 6. Locus of operation for a nonlinear resistor.

Fig. 7. Partitioned nonlinear switched network.

switch port is open and the voltage-controlled switch port is shorted.) Further, the resulting averaged model is a synthesis of the state-space averaged model for the underlying switched converter circuit.

Proof: See Appendix A. Actually, Assumption 4.2 is not required, but results in the simple synthesis rule (19). We give a more general synthesis procedure in the following subsection that is independent of any specific coordinate system.

To obtain the averaged model, one therefore only needs to compute the hybrid immittance H_{22} seen by the switch two-port, and then determine a synthesis for a scaled version of this hybrid immittance function. The linear resistive two-port synthesizing $H_s(d)$ is passive (reciprocal) if the resistive multiport H_R is also passive (reciprocal), since scaling a hybrid matrix by a positive real number preserves these properties. The following example illustrates the use of this result.

Example: Up–Down Converter: Fig. 4 shows a model of an up–down converter that includes parasitic resistance in series with the voltage source. It is straightforward to evaluate the immittance seen by the switch two-port:

$$H_{22} = \begin{bmatrix} r_s & -1 \\ 1 & 0 \end{bmatrix}. \qquad (20)$$

To realize the resistive two-port that replaces the switch network, we synthesize a resistive two-port (see [9]) for $H_s(d) = (d/1 - d)H_{22}$. The resulting averaged circuit is shown in Fig. 5. Note that the averaged circuit includes one more two-terminal resistor than the original switched circuit. This "extra" resistance is required to appropriately realize the one-cycle averaged behavior. Some previous work [14], [18] on this problem resulted in averaged circuit models that did not include this resistance, but simply replaced the switch pair with an ideal transformer. The main contribution of Theorem 4.1 is in streamlining the procedure for constructing the averaged model, and in making explicit the dependence of the averaged switch network on the non-switch circuit elements such as equivalent series resistance (ESR) associated with a voltage source or capacitor.
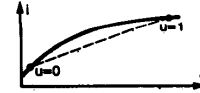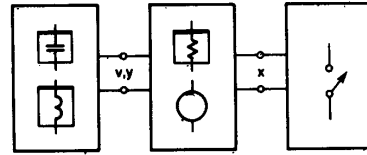
4.2. Averaged Circuit Synthesis with Nonlinear Resistive Elements

As previously discussed, nonlinear reactive elements, linear resistive elements, and dc sources are preserved intact by the one-cycle averaging procedure. The type of element that can present difficulty is a nonlinear resistive element. To see why, consider the current-voltage plot of the operating characteristic for a nonlinear resistor as depicted in Fig. 6. Evidently, the average of the two operating points corresponding to the two different switch configurations is not a point on the operating characteristic for the nonlinear resistor. For this reason, nonlinear resistors need to be treated with care in constructing an averaged circuit. Actually, it is only the nonlinear resistive elements that have discontinuous waveforms that need to be treated differently from the other elements. If the terminal waveforms for a nonlinear resistor are continuous, the waveform trajectory will lie on a connected section of the resistor current-voltage characteristic. Therefore, the nonlinear resistor characteristic will be preserved by the one-cycle averaging operation in the limit of infinitesimally small T, provided the resistor characteristic is smooth. In light of this requirement, we need the following.

Assumption 4.3: All network constitutive relations are C^1.

We shall demonstrate a procedure for constructing an averaged circuit model for a switched power converter that contains nonlinear resistive elements that have discontinuous terminal waveforms. The method lumps the nonlinear resistive element into a multiport network with the switch branches. To carry out the averaged circuit synthesis, Assumptions 4.1 and 4.3 are required.

Consider the partitioned switched circuit of Fig. 7 where all sources are absorbed into the nonlinear resistive multiport. The multiport on the right-hand side of the figure includes all the nonlinear resistive elements that have discontinuous waveforms (switches included as well). For convenience, we shall refer to this multiport as the switch multiport, since it contains at least the switch branches. Let x denote the vector of switch port variables, v denote the vector of inductor currents and capacitor voltages,

and y denote the vector of inductor voltages and capacitor currents. The development will use constraint relations [19] and [25] for the various subnetworks in Fig. 7. We shall construct the constraint relation for the nonlinear resistive multiport (centered in Fig. 7) in two stages. Firstly, denote the constraints imposed by this network on the switch port variables with the relation

$$C_2(v, x) = 0 \tag{21}$$

where the vector of controlling reactive port variables v is viewed as a parameter. Secondly, let the constraints imposed by the resistive multiport on the reactive port variables (v, y) be written in the form

$$-y = C_1(v, x). \tag{22}$$

This can be done as a consequence of Assumption 4.1, which guarantees an explicit solution for y, the vector of inductor voltages and capacitor currents. The constraint imposed by the switch multiport will be represented by the relation

$$Cs_u(x) = 0 \tag{23}$$

where the dependence upon the switch configuration is noted with the subscript u. The composite constraint imposed by the interconnection of the three multiport networks takes the form

$$-y = C_1(v, x)$$
$$0 = C_2(v, x)$$
$$0 = Cs_u(x). \tag{24}$$

The composite constraint relation (24) determines the state-space model since for each value of v, this constraint determines a unique value of y. Further, this set of constraints uniquely determines the vector x of switch variables for each value of v.

With the in-place averaging method, the one-cycle averaged switch variables take the form

$$\bar{x} = (d)x|_{u=1} + (1-d)x|_{u=0} \tag{25}$$

where $x|_u$ is the value of the vector of switch branch variables when the switch configuration is u. Since, by hypothesis, each branch variable in the circuit is well defined for each switch configuration, we can determine the functional form of $x|_u$ in terms of the vector v from the constraints (24), i.e.,

$$x|_u = g_u(v). \tag{26}$$

We conclude that the averaged switch vector $\bar{x}$ assumes the functional form

$$\bar{x} = g_d(\bar{v}) = (d)g_1(\bar{v}) + (1-d)g_0(\bar{v}). \tag{27}$$

Now we require conditions under which we can characterize a manifold in which the vector $\bar{x}$ is constrained to lie. This characterization should be independent of the vector v of the reactive circuit variables. The characterization can be made implicitly via a constraint relation, i.e.,

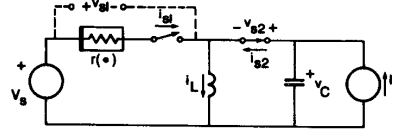$$Cs_d(\bar{x}) = 0 \tag{28}$$

Fig. 8. Up–down converter with nonlinear source resistance.

or with an explicit parametrization. In the previous subsection where we considered the case in which the resistances were linear, this manifold was a subspace of R^4.

Our main result is the following.

Theorem 4.2: A sufficient condition for the construction of an explicit characterization of the manifold in which the averaged switch vector $\bar{x}$ must lie is that the function $C_2(v, x)$ that appears in the second constraint of (24) is separable into two additive terms, i.e.,

$$0 = C_2(v, x) = C_{2v}(v) + C_{2x}(x). \tag{29}$$

Note that a representation $C_2(v, x)$ is not unique, and the separability property may depend upon the particular choice for this representation. However, the statement holds as long as there exists some representation $C_2(v, x)$ that is separable.

Proof: To demonstrate sufficiency, we give a constructive procedure for characterizing the desired manifold. Begin by forming the two functions $g_0(\cdot)$ and $g_1(\cdot)$ which give the explicit solution x for each value of v. Note that these functions take the form (for $u = 0, 1$)

$$g_u(v) = D_u^{-1}\left(\begin{bmatrix} w \\ 0 \end{bmatrix}\right) \tag{30}$$

where

$$D_u(x) = \begin{bmatrix} C_{2x}(x) \\ Cs_u(x) \end{bmatrix} \tag{31}$$

and $w = -C_{2v}(v)$. Next, compute the function $g_d(\cdot)$ according to (27), which takes the form

$$g_d(\bar{v}) = \tilde{g}_d(\bar{w}) = D_d^{-1}\left(\begin{bmatrix} \bar{w} \\ 0 \end{bmatrix}\right)$$
$$= \{(1-d)D_0^{-1} + (d)D_1^{-1}\}\left(\begin{bmatrix} \bar{w} \\ 0 \end{bmatrix}\right). \tag{32}$$

The image of $\tilde{g}_d(\cdot)$ where $\bar{w}$ ranges over R^2 (more properly the subset of R^2 where $\tilde{g}_d(\cdot)$ is well defined) defines the manifold in which the vector $\bar{x}$ of averaged switch port variables must lie. This is typically a two-dimensional manifold embedded in R^4, and is certainly two-dimensional for the extreme cases $d = 0, 1$.

Equation (32) gives an explicit parametrization of the manifold in which the vector $\bar{x}$ of averaged switch port variables must lie. In many cases, it is possible to determine a global implicit representation for this manifold of the form (28) by eliminating the parameter $\bar{w}$ in (32).

Example: Converter with Nonlinear Source Resistance: Consider the up–down converter with nonlinear source resistance that is shown in Fig. 8. In this example, it is possible to lump the nonlinear resistive branch that has

discontinuous waveforms with the switch network, but without increasing the number of ports of this network. This is illustrated in the figure. With the modified port variables, we obtain the following constraint relation imposed by the remainder of the circuit:

$$-i_C = -I_s + i_{s2}$$
$$-v_L = -v_C + v_{s2}$$
$$0 = i_L - i_{s1} - i_{s2}$$
$$0 = -V_s + v_C + v_{s1} - v_{s2}. \tag{33}$$

The first two lines in (33) form the constraint $-y = C_1(v, x)$. The last two lines of (33) form the constraint relation $0 = C_2(v, x)$, which can clearly be expressed in the form $C_{2x}(x) = -C_{2v}(v) = w$, as follows:

$$i_{s1} + i_{s2} = i_L = w_1$$
$$v_{s1} - v_{s2} = V_s - v_C = w_2. \tag{34}$$

To proceed, we form the constraint relations imposed by the modified switch network:

$$Cs_0 : \begin{cases} i_{s1} = 0 \\ v_{s2} = 0 \end{cases} \tag{35}$$

$$Cs_1 : \begin{cases} v_{s1} - r(i_{s1}) = 0 \\ i_{s2} = 0. \end{cases} \tag{36}$$

Next, form the two functions $D_0^{-1}(\cdot)$ and $D_1^{-1}(\cdot)$ by combining (34) and (35) and by combining (34) and (36), respectively. We obtain

$$D_0^{-1}(\cdot) : \begin{cases} i_{s1} = 0 \\ v_{s1} = w_2 \\ i_{s2} = w_1 \\ v_{s2} = 0 \end{cases} \tag{37}$$

$$D_1^{-1}(\cdot) : \begin{cases} i_{s1} = w_1 \\ v_{s1} = r(w_1) \\ i_{s2} = 0 \\ v_{s2} = -w_2 + r(w_1). \end{cases} \tag{38}$$

The function

$$D_d^{-1}(w_1, w_2) = (1 - d) D_0^{-1}(w_1, w_2) + (d) D_1^{-1}(w_1, w_2)$$

gives an explicit parametrization of the desired two-dimensional manifold in terms of the parameters w_1 and w_2. This function takes the form

$$i_{s1} = (d) w_1$$
$$v_{s1} = (1 - d) w_2 + (d) r(w_1)$$
$$i_{s2} = (1 - d) w_1$$
$$v_{s2} = (d)(-w_2 + r(w_1)). \tag{39}$$

The characterization (39) in terms of the variables w_1 and w_2 is an adequate representation of the two-dimensional manifold to which the average switch variables are constrained. However, it is possible to eliminate the parameters w_1 and w_2 by combining the lines of (39) to obtain an
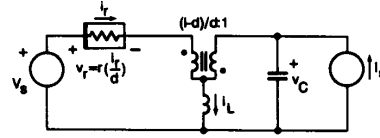

Fig. 9. Average circuit realization for up–down converter with nonlinear source resistance.
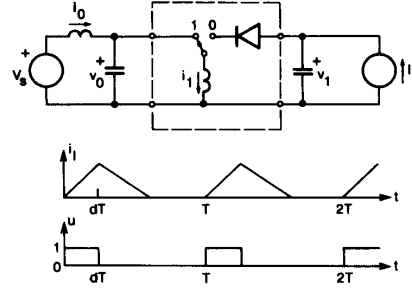

Fig. 10. Model and waveforms for discontinuous conduction mode of up–down converter.

implicit representation of the manifold, i.e., a constraint relation. The constraint relation takes the form

$$0 = (1 - d) i_{s1} - (d) i_{s2}$$

$$0 = (1 - d) v_{s2} + (d) v_{s1} - (d) r \left(\frac{i_{s1}}{d} \right). \tag{40}$$

We can obtain an equivalent hybrid representation for the resistive network described by (40) as follows:

$$i_{s2} = \frac{1 - d}{d} i_{s1}$$

$$v_{s1} = -\frac{1 - d}{d} v_{s2} + r \left(\frac{i_{s1}}{d} \right). \tag{41}$$

The hybrid representation suggests a synthesis involving an ideal transformer and a two-terminal nonlinear resistor. This synthesis is shown in Fig. 9.

The method of circuit averaging developed in this paper can be applied to converters operating in the discontinuous conduction mode, as demonstrated in the following example. This problem was addressed in the paper of Ćuk and Middlebrook [21] using the so-called "hybrid modeling" technique. Our approach is somewhat more systematic. The recent work of Vorperian [16] on this problem also relies on in-place averaging, but proceeds somewhat differently.

Example: Converter Operating in the Discontinuous Conduction Mode: Consider the up–down converter and the typical inductor current waveform for operation in the discontinuous conduction mode shown in Fig. 10. The other state variable waveforms exhibit relatively small ripple, and so are not shown. The diode in the figure is necessary to capture the circuit behavior in the discontinuous conduction mode. In order to apply any averaged

circuit synthesis technique for such a circuit, we need to recognize that a switching converter operating in the discontinuous conduction mode is governed by a reduced order state-space averaged model. This statement can be justified by the idea that an averaged model should have the same order as an *exact* sampled-data model for the underlying circuit. (Ideally, sampled-data models derived from the averaged circuit and the underlying circuit should be identical.) Since the L_1 inductor current is identically zero during a portion of each cycle, a sampled-data model for the circuit would not include the inductor current as a state variable. Therefore, in our scheme, we treat this inductor as a nonlinear resistive element. In contrast, the averaged circuit model of Vorperian [16] retains the inductor whose current enters the discontinuous conduction mode. This practice may be considered nonphysical if one attempts to identify a sampled-data model for the resulting averaged circuit with a sampled-data model for the underlying switched circuit.

Our method proceeds by lumping the L_1 inductor with the switch branches and the diode into a modified two-port switch network as shown in Fig. 10. With the indicated partitioning, it is now straightforward to apply our procedure. The constraint $C_2(v, x) = 0$ takes the form

$$v_{s1} - v_0 = 0$$
$$v_{s2} - v_1 = 0. \qquad (42)$$

This constraint clearly satisfies the separability condition, and can easily be expressed in the form $C_{2x}(x) = -C_{2v}(v) = w$ as follows:

$$v_{s1} = v_0 = w_1$$
$$v_{s2} = v_1 = w_2. \qquad (43)$$

The next step is to obtain the constraints imposed by the extracted (and modified) switch network for each of the two switch configurations. Since the inductor current i_1 varies significantly over each cycle, we shall compute an averaged constraint for each of the two configurations. When the switch is in the 0 position during an interval $[t_j, t_j + dT)$, the current $i_{s2} = 0$ and the current i_{s1} is equal to the L_1 inductor current. The average value of the latter current over this interval can readily be seen to be $(v_0 dT / 2 L_1)$ from the form of the waveform in Fig. 10. Hence we obtain the averaged constraint for this interval as

$$Cs_0 : \begin{cases} i_{s1} - \dfrac{v_{s1} dT}{2 L_1} = 0 \\ i_{s2} = 0. \end{cases} \qquad (44)$$

With a similar calculation for the interval $[t_j + dT, t_j + T)$ when the switch is in the 1 position, we obtain

$$Cs_1 : \begin{cases} i_{s1} = 0 \\ i_{s2} + \dfrac{v_{s1}^2 d^2 T}{2 v_{s2} L_1 (1 - d)} = 0. \end{cases} \qquad (45)$$

Next, we form the two functions $D_0^{-1}(\cdot)$ and $D_1^{-1}(\cdot)$ by combining (43) and (44) and by combining (43) and (45), respectively.

$$D_0^{-1}(\cdot) : \begin{cases} v_{s1} = w_1 \\ v_{s2} = w_2 \\ i_{s1} = \dfrac{w_1 dT}{2 L_1} \\ i_{s2} = 0 \end{cases} \qquad (46)$$

$$D_1^{-1}(\cdot) : \begin{cases} v_{s1} = w_1 \\ v_{s2} = w_2 \\ i_{s1} = 0 \\ i_{s2} = -\dfrac{w_1^2 d^2 T}{2 w_2 L_1 (1 - d)}. \end{cases} \qquad (47)$$

We can then form the function $D_d^{-1}(w_1, w_2)$ as in the previous example, i.e.,

$$D_d^{-1}(\cdot, \cdot) : \begin{cases} v_{s1} = w_1 \\ v_{s2} = w_2 \\ i_{s1} = \dfrac{w_1 d^2 T}{2 L_1} \\ i_{s2} = -\dfrac{w_1^2 d^2 T}{2 w_2 L_1}. \end{cases} \qquad (48)$$

The function $D_d^{-1}(w_1, w_2)$ gives an explicit parametrization of the manifold in which the modified switch port variables are constrained to lie. It is possible to obtain a voltage controlled representation for this two-port network by eliminating w_1 and w_2 in (48). This representation takes the form

$$i_{s1} = \dfrac{v_{s1} d^2 T}{2 L_1}$$

$$i_{s2} = -\dfrac{v_{s1}^2 d^2 T}{2 v_{s2} L_1}. \qquad (49)$$

With this type of representation for a resistive two-port network that replaces the modified switch network in Fig. 10, we readily obtain the averaged circuit representation shown in Fig. 11.

It is of interest that the resistive two-port model (49) is an incrementally passive model. This can be seen by evaluating the Jacobian matrix for this model, i.e.,

$$\left[\dfrac{di_s}{dv_s} \right] = \begin{bmatrix} \dfrac{d^2 T}{2 L_1} & 0 \\ -\dfrac{v_{s1} d^2 T}{v_{s2} L_1} & \dfrac{v_{s1}^2 d^2 T}{2 v_{s2}^2 L_1} \end{bmatrix}. \qquad (50)$$

This Jacobian matrix is evidently positive semi-definite (where it is well defined), leading to the conclusion that the two-port is incrementallly passive.
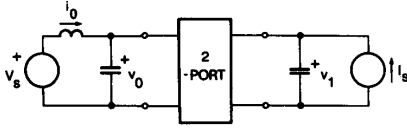
Fig. 11. Average circuit model for discontinuous conduction mode.

V. Summary

We have illustrated a systematic approach for synthesizing averaged circuit models for switching converters. The averaged circuit models that are obtained are realizations of the state-space averaged models for the underlying circuits, and further, resemble very closely the underlying circuits. None of the methods for averaged circuit synthesis that are presently available in the literature offers as systematic an approach to averaged circuit synthesis. Further, our approach to averaged circuit synthesis is applicable to circuits whose non-switch elements may be nonlinear. This feature is not shared by any previous work on averaged circuit models.

Appendix A
Proof of Theorem 4.1

Define the controlling port variable of the reactive multiport to be the inductor currents and the capacitor voltages (elements of vector x_1), the controlling port variables of the source multiport to be voltages for voltage sources and currents for current sources (elements of vector x_3), and select one of the two ports of the switch network to be current-controlled and the other to be voltage-controlled, as shown in Fig. 3.

Partition H_R to reflect the three sets of ports to which it is connected, i.e.,

$$H_R = \begin{bmatrix} H_{11} & H_{12} & H_{13} \\ H_{21} & H_{22} & H_{23} \\ H_{31} & H_{32} & H_{33} \end{bmatrix} \quad (51)$$

where the first set of ports are those connected to the reactive network, the second set consists of the ports connected to the switch network, and the third set corresponds to the ports connected to the source network. For the two-port switch network, with the controlling variables and switch positions ($u = 0, 1$) indicated in Fig. 3, we obtain for $u = 0$

$$H_s(0) = \begin{bmatrix} 0 & 0 \\ 0 & 0 \end{bmatrix}. \quad (52)$$

For $u = 1$, the hybrid representation is not well defined, but it is clear that the controlling port variables are constrained to be zero, i.e., $x_2 = 0$.

A first step in deriving the required constitutive relation is to determine the explicit solution for the vector of switch port variables for each switch configuration, i.e.,

$$\begin{bmatrix} x_2|_u \\ y_2|_u \end{bmatrix}$$

where $x_2|_u$ is the vector of controlling port variables and $y_2|_u$ is the vector of complementary noncontrolling port variables. (The subscript u indicates which switch configuration is present.) For this purpose, consider the application of the network constraints (KCL and KVL) at the switch ports, i.e.,

$$H_{21}x_1 + [H_s(u) + H_{22}]x_2|_u + H_{23}x_3 = 0. \quad (53)$$

With (53) and the relations imposed by the hybrid model H_R for the resistive subnetwork in Fig. 3, it is possible to solve for $x_2|_u$ and $y_2|_u$. In particular, for $u = 0$, we have

$$x_2|_{u=0} = -H_{22}^{-1}[H_{21}x_1 + H_{23}x_3]$$

$$y_2|_{u=0} = 0. \quad (54)$$

The first line in (54) is obtained by noting that $H_s(0) = 0$ in (53), and that H_{22}^{-1} must exist, or else there would not exist an unique solution $x_2|_{u=0}$. The second line is a simple consequence of the fact that $H_s(0) = 0$, or equivalently, that $y_2|_{u=0}$ is constrained to be zero by the switch network. For $u = 1$, we obtain

$$x_2|_{u=1} = 0$$

$$y_2|_{u=1} = H_{21}x_1 + H_{23}x_3. \quad (55)$$

The first line in (55) is a consequence of the constraint imposed by the switch network, and the second line is obtained by considering the hybrid relationship for the resistive subnetwork.

With the above formulas for the switch port variables in each switch configuration, it is possible to determine the one-cycle averaged values for the switch port variables, i.e.,

$$\bar{x}_2 = (1-d)x_2|_{u=0} + (d)x_2|_{u=1} = -(1-d)H_{22}^{-1}w$$

$$\bar{y}_2 = (1-d)y_2|_{u=0} + (d)y_2|_{u=1} = (d)w \quad (56)$$

where $w = [H_{21}x_1 + H_{23}x_3]$. Note that (56) gives an explicit parametrization of the subspace of R^4 that contains the vector of one-cycle averaged switch port variables. This subspace is parametrized by the vector $w \in R^2$. (This type of parametrization is essential in the case where nonlinear resistive elements are present in the switched circuit. See Section 4.2.) In the actual operation of the circuit, the port variables may not attain any arbitrary point in the subspace parametrized by w in (56), since evidently w may not assume any arbitrary value in R^2. For our purposes, it is adequate to characterize a two-port resistive network that constrains its port variables to lie in the defined subspace. Such a characterization is sufficient because it constrains the averaged switch port variables as required in the averaged circuit. It will be demonstrated that such a characterization will result in an averaged circuit that realizes the state-space averaged model.

A more familiar functional relationship can be obtained by elimination of w in (56), i.e.,

$$\bar{y}_2 = -\frac{d}{1-d}H_{22}\bar{x}_2 \quad (57)$$

for $d \neq 1$. The relationship (57) suggests that the two-port

switch network should be replaced in the averaged circuit by a resistive two-port with hybrid representation given by (19), i.e.,

$$H_s(d) = \frac{d}{1-d} H_{22} \qquad (58)$$

for $d \neq 1$. (A sign reversal is required to account for the opposing polarities of the noncontrolling port variables of the switch and resistive subnetworks in the original switched circuit.)

To see that the resulting averaged circuit model is a realization of the state-space averaged model, consider the following explicit solution for $\bar{y}_1$, the negative of the averaged vector of inductor voltages and capacitor currents (the noncontrolling reactive port variables):

$$\bar{y}_1 = H_{11}\bar{x}_1 + H_{12}\bar{x}_2 + H_{13}\bar{x}_3$$

$$= H_{11}\bar{x}_1 - (1-d)H_{12}H_{22}^{-1}\big[H_{21}\bar{x}_1 + H_{23}\bar{x}_3\big] + H_{13}\bar{x}_3 \qquad (59)$$

where the form of $\bar{x}_2$ in the second line of (59) is obtained from (56). The state-space averaged model can be obtained from (59) by simply writing

$$\bar{q}_1' = -\bar{y}_1 \qquad (60)$$

since $\bar{y}_1$ can in turn be written in terms of $\bar{x}_1 = Q^{-1}(\bar{q}_1)$ and $\bar{x}_3$ using (59). This is readily verified to be the form of the state-space averaged model, by noting that it varies with d on the chord connecting the two extreme state-space models obtained by solving the network equations under $u = 0$ and $u = 1$.

REFERENCES

[1] J. R. Wood, "Power conversion in electrical networks," Ph.D. dissertation, EECS Dept., MIT, 1973.

[2] G. C. Verghese, M. E. Elbuluk, and J. G. Kassakian, "A general approach to sampled-data modeling for power electronic circuits," IEEE Trans. Power Electronics, pp. 76–89, Apr. 1986.

[3] K. D. T. Ngo, "Topology and analysis in PWM inversion, rectification, and cycloconversion," Ph.D. dissertation, EE Dept., California Tech. Univ., 1984.

[4] R. W. Brockett and J. R. Wood, "Electrical networks containing controlled switches," in Addendum to Proc. IEEE Symp. Circuit Theory, Apr. 1974.

[5] R. D. Middlebrook and S. Cuk, "A general unified approach to modelling switching power converter stages," IEEE PESC Record, pp. 18–34, 1976.

[6] H. Sira-Ramirez, "Sliding motions in bilinear switched networks," IEEE Trans. Circuits Syst., vol. CAS-34, pp. 919–933, Aug. 1987.

[7] M. Hasler and J. Neirynck, Nonlinear Circuits. Norwood, MA: Artech House, 1986.

[8] J. L. Wyatt, Jr., L. O. Chua, J. W. Gannett, I. C. Goknar, and D. N. Green, "Energy concepts in the state-space theory of nonlinear n-ports: Part I—Passivity," IEEE Trans. Circuits Syst., vol. CAS-38, Jan. 1981.

[9] B. D. O. Anderson and S. Vongpanitlerd, Network Analysis and Synthesis: A Modern Systems Theory Approach. Englewood Cliffs, NJ: Prentice-Hall, 1973.

[10] C. A. Desoer and M. Vidyasagar, Feedback Systems: Input–Output Properties. New York: Academic, 1975.

[11] J. L. Wyatt, Jr., L. O. Chua, J. W. Gannett, I. C. Goknar, and D. N. Green, "Energy concepts in the state-space theory of nonlinear n-ports: Part II—Losslessness," IEEE Trans. Circuits Syst., vol. CAS-29, July 1982.

[12] F. W. Warner, Foundations of Differentiable Manifolds and Lie Groups. New York: Springer-Verlag, 1983.

[13] S. Cuk and R. D. Middlebrook, Modeling, Analysis, and Design of Switching Converters, NASA Rep. CR-135174.

[14] R. Tymerski, V. Vorperian, F. C. Lee, and W. Baumann, "Nonlinear modeling of the PWM switch," IEEE PESC Record, 1988.

[15] V. Vorperian, "Simplify your PWM converter analysis using the model of the PWM switch, Part I: Continuous conduction mode," Current (Virginia Polytech Newsletter), pp. 8–13, Fall 1988.

[16] ___, "Simplify your PWM converter analysis using the model of the PWM switch, Part II: Discontinuous conduction mode," Current (Virginia Polytech Newsletter), pp. 6–12, Spring 1989.

[17] Y. S. Lee, "A systematic and unified approach to modeling switches in switch-mode power supplies," IEEE Trans. Ind. Electron., vol. IE-32, pp. 445–448, Nov. 1985.

[18] G. W. Wester and R. D. Middlebrook, "Low frequency characterization of switched dc-dc converters," IEEE PESC Record, 1972.

[19] L. O. Chua and P. M. Lin, Computer Aided Analysis of Electronic Circuits: Algorithms and Computational Techniques. Englewood Cliffs, NJ: Prentice-Hall, 1975.

[20] J. G. Kassakian, M. F. Schlecht, and G. C. Verghese, Principles of Power Electronics. Springfield, MA: Addison-Wesley, 1991.

[21] S. Cuk and R. D. Middlebrook, "A general unified approach to modeling switching converters in discontinuous conduction mode," IEEE PESC Record, pp. 36–57, 1977.

[22] Y. P. Tsividis, "Analytical and experimental evaluation of a switched-capacitor filter and remarks on the resistor/switched capacitor correspondence," IEEE Trans. Circuits Syst., vol. CAS-26, pp. 140–144, Feb. 1979.

[23] J. A. Nossek and H. Weinrichter, "Equivalent circuits for switched-capacitor networks including recharging devices," IEEE Trans. Circuits Syst., vol. CAS-27, pp. 539–544, June 1980.

[24] A. Knob and R. Dessoulavy, "Analysis of switched-capacitor networks in the frequency domain using continuous-time two-port equivalents," IEEE Trans. Circuits Syst., vol. CAS-28, pp. 947–953, Oct. 1981.

[25] L. O. Chua, Lecture Notes for Network Theory, EECS 223, Univ. California, Berkeley, 1980.

[26] J. K. Zuidweg, "Every passive time-invariant linear n-port has at least one 'H matrix'," IEEE Trans. Circuit Theory, vol. CT-12, pp. 131–132, Mar. 1965.

[27] B. D. O. Anderson, R. W. Newcomb, and J. K. Zuidweg, "On the existence of H matrices," IEEE Trans. Circuit Theory, vol. CT-13, pp. 109–110, Mar. 1966.

[28] L. C. Fu, M. Bodson, and S. S. Sastry, "New stability theorems for averaging and their application to the convergence analysis of adaptive identification and control schemes," in Proc. 24th IEEE Conf. Dec. and Control, pp. 473–477, 1985.

[29] J. Ezzine and A. H. Haddad, "Error bounds in the averaging of hybrid systems," IEEE Trans. Automat. Contr., vol. 34, pp. 1188–1192, Nov. 1989.

[30] J. L. Wyatt, Jr., "Lectures on nonlinear circuit theory," VLSI Memo 84-158, revised Aug. 1984. (All VLSI Memos are available from the Microsystems Research Center, Room 39-321, MIT, Cambridge, MA 02139, or from the author.

[31] S. R. Sanders, "Nonlinear control of switching power converters," Ph.D. dissertation, EECS Dept., MIT, 1989.

[32] S. R. Sanders, J. M. Noworolski, X. Z. Liu, and G. C. Verghese, "Generalized averaging method for power conversion circuits," IEEE PESC Record, 1990, and in IEEE Trans. Power Electron., Apr. 1991.

[33] A. F. Witulski and R. W. Erickson, "Extension of state-space averaging to resonant switches and beyond," IEEE Trans. Power Electron., vol. 5, pp. 98–109, Jan. 1990.

[34] J. Xu and J. Yu, "Time-averaging equivalent circuit analysis of a resonant switching converter," Int. J. Electron., vol. 67, pp. 937–948, 1989.

[35] R. Steigerwald, "A comparison of half-bridge resonant converter topologies," IEEE Trans. Power Electron., vol. 3, pp. 174–182, Apr. 1988.

[36] C. T. Rim and G. H. Cho, "Phasor transformation and its application to the dc/ac analyses of frequency phase-controlled series resonant converters (SRC)," IEEE Trans. Power Electron., vol. 5, pp. 201–211, Apr. 1990.

[37] P. T. Krein, J. Bentsman, R. M. Bass, and B. L. Lesieutre, "On the use of averaging for the analysis of power electronic systems," IEEE Trans. Power Electron., vol. 5, pp. 182–190, Apr. 1990.

[38] J. M. Noworolski and S. R. Sanders, "Generalized in-place circuit averaging," presented at IEEE Applied Power Electronics Conference (APEC), Mar. 1991.

Seth R. Sanders received B.S. degrees in electrical engineering and physics from MIT, Cambridge, MA in 1981, and received the S.M. and Ph.D. degrees in electrical engineering in 1985 and 1989, respectively, also from MIT.

He is presently an Assistant Professor in the Department of Electrical Engineering and Computer Sciences at the University of California at Berkeley. His research interests are in the area of nonlinear control systems and circuits, and particularly in applications to power electronics, electromechanical systems, and power systems.
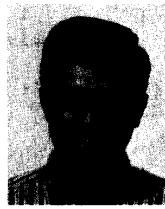
George C. Verghese received the B.Tech degree from the Indian Institute of Technology, Madras, in 1974, the M.S. degree from the State University of New York, Stony Brook, in 1975, and the Ph.D. degree from Stanford University, CA, in 1979, all in electrical engineering.

He is Associate Professor of Electrical Engineering and a member of the Laboratory for Electromagnetic and Electronic Systems at the Massachusetts Institute of Technology, which he joined in 1979. His research interests are in the areas of systems, control, and estimation, especially as applied to power electronics, electrical machines, and bulk power systems.

Dr. Verghese is an Associate Editor of *Automatica* and of the IEEE Transactions on Automatic Control. He is co-author (with J. G. Kassakian and M. F. Schlecht) of *Principles of Power Electronics*, Addison-Wesley, 1991.